

Article

Sll0528, a Site-2-Protease, Is Critically Involved in Cold, Salt and Hyperosmotic Stress Acclimation of Cyanobacterium *Synechocystis* sp. PCC 6803

Haijin Lei, Gu Chen *, Yuling Wang, Qinglong Ding and Dong Wei

College of Light Industry and Food Sciences, South China University of Technology, 381 Wushan Road, Guangzhou 510641, China; E-Mails: lei_hai_jin@163.com (H.L.); wang.yulingwyl@163.com (Y.W.); dingql21@126.com (Q.D.); fewd304@scut.edu.cn (D.W.)

* Author to whom correspondence should be addressed; E-Mail: chengu@scut.edu.cn;
Tel./Fax: +86-20-8711-3848.

External Editor: Bing Yan

Received: 30 September 2014; in revised form: 21 November 2014 / Accepted: 25 November 2014 /
Published: 8 December 2014

Abstract: Site-2-proteases (S2Ps) mediated proteolysis of transmembrane transcriptional regulators is a conserved mechanism to regulate transmembrane signaling. The universal presence of S2P homologs in different cyanobacterial genomes suggest conserved and fundamental functions, though limited data has been available. Here we provide the first evidence that Sll0528, a site-2-protease in *Synechocystis* sp. PCC 6803 is crucial for salt, cold and hyperosmotic stress acclimation. Remarkable induction of *sll0528* gene expression was observed under salt, cold and hyperosmotic stress, much higher than induction of the other three S2Ps. Knock-out of *sll0528* gene in wild type *Synechocystis* sp. PCC 6803 increased their sensitivity to salt, cold and hyperosmotic stress, as revealed by retarded growth, reduced pigments and disrupted photosystems. The *sll0528* gene was induced to a much smaller extent by high light and mixotrophic growth with glucose. Similar growth responses of the *sll0528* knockout mutant and wild type under high light and mixotrophic growth indicated that *sll0528* was dispensable for these conditions. Recombinant Sll0528 protein could cleave beta-casein into smaller fragments. These results together suggest that the Sll0528 metalloprotease plays a role in the stress response and lays the foundation for further investigation of its mechanism, as well as providing hints for the functional analysis of other S2Ps in cyanobacteria.

Keywords: *Synechocystis* sp. PCC 6803; site-2-proteases; SII0528; cold stress; salt stress; hyperosmotic stress; RT-qPCR; knock-out mutant; *in vitro* protease activity

1. Introduction

As the oldest and most abundant photosynthetic organisms, cyanobacteria (blue-green algae) play essential roles in ecology and biogeochemistry. Their stress responses are good examples for indicating how organisms adapt to an ever-changing environment. Recently, cyanobacteria have attracted considerable attention as a sustainable resource of energy and biomolecules due to their photosynthetic conversion of CO₂, water and sunlight into bio-based fuels and chemicals [1–3]. Therefore, it is important to understand the stress response of cyanobacteria for scientific interests as well as for biotechnological applications.

In cyanobacterium *Synechocystis* sp. PCC 6803 (hereafter *Synechocystis*), two-component regulatory systems, serine/threonine protein kinases, and transcription factors, as well as RNA polymerase sigma factor (σ) subunits are revealed as stress sensors and signal transducers during stress response [4]. Nonetheless, many questions remain. For example, how are sigma factors activated during the stress response? Among the known mechanisms of transmembrane signaling, the Site-2-proteases (S2Ps) mediated proteolysis of transmembrane transcriptional regulators is widespread and conserved among different organisms [5]. Site-2 proteases are named after the founding member of this protease family, human S2P. Human S2P activates cholesterol and fatty acid biosynthesis by cleaving transcription factor SREBP (Sterol Regulatory Element Binding Protein) after site-1 protease (S1P) cleavage [6,7]. S2P homologs are multiple transmembrane proteins with a conserved HExxH active motif within a transmembrane domain and an NPDG motif in another transmembrane domain. S2Ps are widely identified in bacteria, fungi, plant and animals, suggesting their conserved and essential functions in signal transduction [5,8]. We have characterized S2P homologs in photosynthetic organisms, such as EGY1 and EGY2 in *Arabidopsis*, and Slr0643 in *Synechocystis* [9–12]. EGY1, a chloroplast membrane-bound metalloprotease, is required for thylakoid grana development and accumulation of chlorophyll and chlorophyll a/b binding proteins [9]. EGY1 is also involved in regulation of endodermal plastid size and number, as well as the stimulatory effect of ethylene on hypocotyl gravitropism [13]. EGY2, another chloroplast-located *Arabidopsis* S2P, plays a role in hypocotyl elongation [10]. Slr0643 is essential for acid acclimation in *Synechocystis* probably through the activation of SigH [12].

At least one, and usually more than one S2P was identified in all of the presently available cyanobacterial genomes, including the reduced genomes from marine picoplanktonic strains such as *Synechococcus* and *Prochlorococcus*. The universal presence of S2P homologs in different cyanobacterial genomes suggest conserved and fundamental functions, though limited data has been available. Recently five putative S2Ps in *Anabaena variabilis* were reported [14], but their physiological functions remain enigmatic, and none of their *in vivo* substrates are revealed.

Thus, here in this study, we first investigated the gene expression profile of four S2Ps (SII0528, Slr0643, SII0862 and Slr1821) of *Synechocystis* under five conditions, namely salt, cold, hyperosmotic

stress, high light and mixotrophic growth. Then the function of *sll0528*, the gene which was the most dramatically induced upon stress, was further explored through its knockout mutant and *in vitro* protease activity assay. Results indicated that the metalloprotease Sll0528 plays an essential role in salt, cold and hyperosmotic stress acclimation of *Synechocystis*.

2. Results and Discussion

2.1. Expression Profile of S2Ps under Different Conditions

Gene expression profiles of four S2P genes of *Synechocystis*, *sll0528*, *slr0643*, *sll0862* and *slr1821*, were investigated under five conditions, namely salt, hyperosmotic stress, cold, high light and mixotrophic growth (Figure 1).

Under salt stress with 854 mM NaCl, expression level of *sll0528* kept increasing intensively from 0.25 to 6 h, with an expression ratio of more than 50-fold at 4 to 6 h (Figure 1a). The induction patterns of *slr0643*, *sll0862* and *slr1821* genes were similar, with maximal induction at 0.5 h. But their maximal induction was less than 3-fold and much smaller than the induction in *sll0528*. More than forty-fold induction of *sll0528* was previously identified when incubated with 500 mM NaCl for 30 min, 684 mM NaCl for 2 h or 500 mM NaCl for 20 min [15–17]. Such consistent and remarkable induction of *sll0528* at different salt concentrations and different experimental duration suggested that *sll0528* was actively involved in salt stress acclimation.

Prompt and sharp *sll0528* induction was observed under hyperosmotic stress generated by 0.5 M sorbitol (Figure 1b). Its expression peaked as 100-fold at 0.25 h and gradually decreased to around the basal level at 6 h. The *slr1821* expression was also enhanced with a maximum 5.5-fold upregulation at 1 h. Hyperosmotic induction of *sll0528* was reported previously at a varied extent, as 4-, 20- or 40-fold induction upon 0.5 M sorbitol in different reports [15,18,19]. Different extents of sorbitol induction might be due to different experimental conditions used by different groups and different time points of observation upon sorbitol treatment.

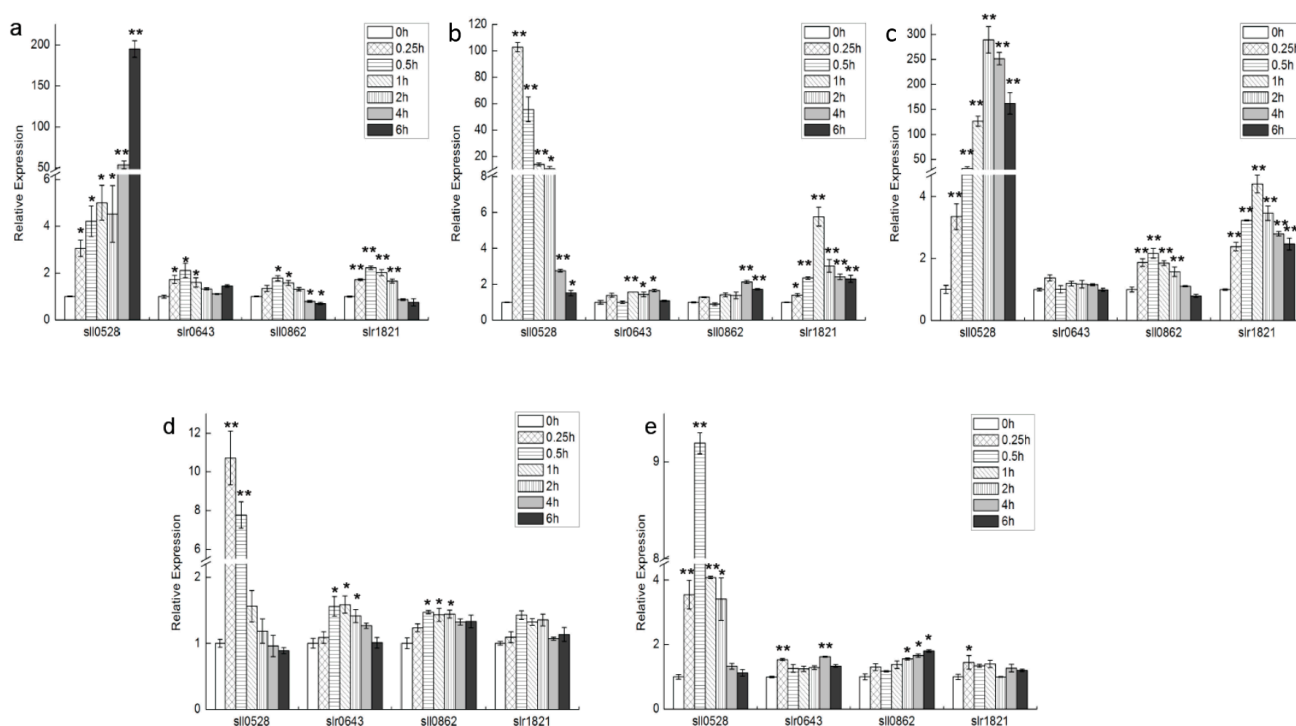
Upon transferring to 4 °C, a huge induction was observed in *sll0528* expression, with more than 100-fold upregulation from 1 to 6 h, which peaked at around 2–4 h (Figure 1c). Compared with *sll0528*, *sll0862* and *slr1821* have relatively small but significant upregulation, with maximal induction at 0.5 and 1 h respectively. The relative expression level of *slr0643* was almost unchanged at 4 °C. Compared with the literature, induction of *sll0528* observed here was much higher than the previously reported three times upregulation after transfer from 34 to 22 °C [20]. Fourier transform infrared spectrometry indicated that lipids in plasma membranes were rigidified with decreases in temperature, and cold inducibility of *sll0528* was enhanced upon rigidification of membrane lipids by knocking out the fatty acid desaturases [20]. Thus it was reasoned that higher rigidification of membrane upon lower temperature in our study might partially explain the enhanced *sll0528* inducibility at 4 °C. Further, the sensitivity of *sll0528* induction to temperature decrease might imply its active role in cold stress acclimation.

Upon exposure to high light (200 $\mu\text{mol}\cdot\text{photons}\cdot\text{m}^{-2}\cdot\text{s}^{-1}$), an about 10-fold induction was observed in the *sll0528* gene at 0.25 h, but the expression then dropped to basal level at around 2 h (Figure 1d). Compared with the more than 100-fold induction of *sll0528* under cold, salt and hyperosmotic stress, the high light induction of *sll0528* was relatively small and transient. At the same time, only slight

induction (less than 1.6-fold) was found in other S2Ps during 0.5 to 2 h, indicating they might not be the primary responsive elements for high light adaption.

Similar with the situation upon high light, a relative small and transient induction of *sll0528* was found in response to glucose mixotrophism (2.5 mM glucose) (Figure 1e). Its expression peaked at 0.5 h as 9-fold and decreased back to basal level at 4 h.

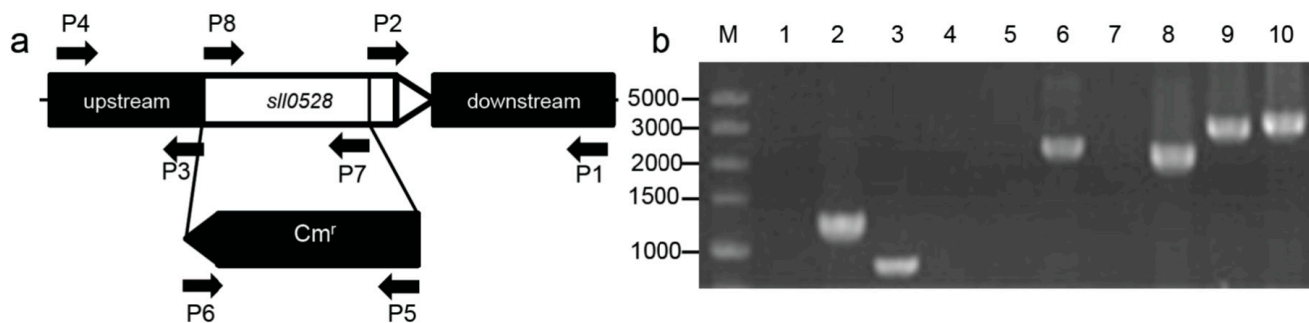
Figure 1. Transcriptional profiles of four S2P homologs under different conditions. Time course expression profile of *sll0528*, *slr0643*, *sll0862* and *slr1821* genes under salt (a); hyperosmotic stress (b); cold (c); high light (d) and mixotrophic growth (e) were analyzed by quantitative real-time RT-PCR. Significant differences were indicated as * for $p < 0.05$, and ** for $p < 0.01$.



2.2. Construction of the *sll0528* Knockout Mutant

Due to the strongest induction of *sll0528* gene expression with different stress treatments, it was selected for detailed characterization. A knockout mutant was generated for further physiological characterization under different stress conditions. The *sll0528* gene was disrupted by replacing most of its coding region with a chloramphenicol resistance cassette (Cm^r) (Figure 2a). After intensive selection under photoautotrophic growth, a completely segregated mutant of *sll0528* was obtained and verified by PCR and sequencing of PCR products (Figure 2b). The corrected insertion of chloramphenicol resistance cassette (Cm^r) was further confirmed by Thermal asymmetric interlaced PCR (TAIL-PCR). In searching for the flanking region of the inserted Cm^r gene, only the upstream and downstream regions of the *sll0528* gene were retrieved in TAIL-PCR using different degenerate primers. RT-PCR in mutants indicated that no *sll0528* transcripts could be detected and confirmed that the *sll0528* gene was successfully disrupted (data not shown).

Figure 2. Construction of the *sll0528* mutant. (a) The coding region of the *sll0528* gene was replaced with a chloramphenicol resistance gene cassette (Cm^r) obtained from pACYC184. The arrows P1 to P8 indicated the primers used in PCR verification; (b) PCR verification of the *sll0528* mutant. Template was genomic DNA from wild type (lanes 1, 3, 5, 7, 9) or *sll0528* mutant (lanes 2, 4, 6, 8, 10). Primers used as indicated (a) were P5 + P6 (lanes 1, 2), P7 + P8 (lanes 3, 4), P1 + P6 (lanes 5, 6), P4 + P5 (lanes 7, 8) and P1 + P4 (lanes 9, 10). PCR products were sequenced to confirm their authenticity.



2.3. Varied Phenotype of *sll0528* Mutant under Different Conditions

The *sll0528* mutant grew as well as wild type under optimum culture condition (Figures 3a and 4a), suggesting the Sll0528 protein was dispensable for cell viability at optimized conditions. But the *sll0528* mutant displayed varied responses to different conditions.

2.3.1. Sll0528 Is Crucial for Acclimation to Salt Stress

The acclimation of wild type and the *sll0528* mutant upon salt stress was investigated under 0.5–1.2 M NaCl (Figure 3a). Addition of 0.5 M NaCl in BG11 medium only impeded the growth of wild type insignificantly. But NaCl of 0.6 to 0.9 M notably retarded its growth and 1.2 M NaCl completely blocked the growth of wild type. The growth rate of wild type was nearly halved at 0.9 M NaCl. Compared with wild type, the *sll0528* mutant was much more sensitive to salt stress (Figure 3a). NaCl of 0.5 M impeded the mutant growth significantly, and growth rate under 0.6 M NaCl was less than half of the control. No growth was detected in the mutant even under 0.9 M NaCl.

Furthermore, the whole-cell absorption spectra of wild type and mutant were compared (Figure 3b). The representative absorption peaks for chlorophyll (440 and 680 nm), carotenoids (480–500 nm) and phycocyanin (600–650 nm) were lower in wild type upon salt stress. However, the reduction was much more severe in the *sll0528* mutant. This indicated that accumulation of light-harvesting antenna pigment was severely affected. Further extraction and analysis of chlorophyll content revealed that the reduction of chlorophyll under salt stress was much more severe in mutant than wild type (Figure 3c) and it was consistent with absorption spectra results. Then the fluorescence properties of photosystem I (PSI) and II (PSII) were analyzed by 77 K fluorescence spectroscopy. Excitation of chlorophyll at 435 nm resulted in emission peaks at 685, 695 and 725 nm corresponding to PSII-CP43, PSII-CP47 and PSI, respectively. The PSI/PSII ratio was similar between wild type and mutant under optimal condition. However, the salt induced decrease of the PSI/PSII ratio was much bigger in mutant than in wild type (Figure 3d), suggesting that the photosystem in the *sll0528* mutant was seriously impaired upon salt

stress. The seriously impaired photosystems in the *sll0528* mutant might partially explain its retarded, even halted growth under NaCl concentrations that were tolerated by the wild type.

Marin *et al.* [16] reported that no significant reduction in salt resistance was observed in the completely segregated *sll0528* mutants. The distinction with our observation might be due to different salt concentration and culture condition used or different genomic background of the mutant. Re-sequencing of *Synechocystis* had revealed the genomic diversity among different strains used around the world [21–23].

Salt stress is one of the environmental factors that limit growth and productivity of organism. As reviewed, so far the mechanisms known for cyanobacteria salt acclimation involve active extrusion of toxic inorganic ions and accumulation of compatible solutes, mainly through *de novo* synthesis [24]. Recently, exopolysaccharides were also suggested in the protection against salt stress [25]. And several stress sensors or signal transducers, such as two-component regulatory systems (Hik/Rre-pair), transcription factors, and RNA polymerase sigma factor (σ) were suggested to contribute to salt acclimation [24,26]. Disruption of the *sll0528* gene remarkably increased the sensitivity of *Synechocystis* to salt stress, which implied that functional Sll0528 protein was crucial for efficient salt acclimation. Research is ongoing in our lab to explore how the functional Sll0528 protein cooperates with the known sensors and signal transducers in salt acclimation.

2.3.2. Sll0528 Is Indispensable for Acclimation to Hyperosmotic Stress

Hyperosmotic stress generated by 0.5 M sorbitol impeded the growth of wild type, while the *sll0528* mutant was more sensitive to 0.5 M sorbitol and grew even more slowly (Figure 4a). Whole-cell absorption spectra of wild type and mutant 24 h under 0.5 M sorbitol indicated the remarkable change in the mutant (Figure 4b). Only slight reduction of carotenoids was found in wild type upon hyperosmotic stress, while dramatic reduction of chlorophyll, carotenoids and phycocyanin were found in the mutant (Figure 4b). The nearly flat absorption spectra of the mutant indicated loss of the characteristic photosynthetic pigment and severely impaired photosystems, which were correlated with its disrupted cell growth (Figure 4).

There is some overlap in the acclimation to salt and hyperosmotic stress since both of them increase the water potential inside the cell. But hyperosmotic stress does not generate as much ionic stress as salt stress. It was reported that hyperosmotic stress utilized the identical Hik-Rre two component systems as salt stress in perception and signal transduction, but regulated individual genes to different extents [17,18]. Here in our studies, increased sensitivity was found in the *sll0528* mutant to both salt and hyperosmotic stress (Figures 3 and 4). Whether they are due to the same mechanism awaits further investigation.

Figure 3. Increased sensitivity of *slI0528* mutant to salt stress. (a) Growth curve of wild type (WT) and *slI0528* mutant ($\Delta slI0528$) at different concentration of NaCl (0.5, 0.6, 0.7, 0.9, and 1.2 M respectively). Significant differences were observed between mutant and wild type from the 2nd day to 5th day at NaCl of 0.5, 0.6, 0.7 and 0.9 M ($p < 0.05$). Initial OD₇₃₀ was 0.1. Each data point represents the mean of at least three independent biological replicates, and the error bars denote SD; (b) Absorption spectra of wild type and *slI0528* mutant 24 h after transfer to 0.5 M NaCl, normalized to OD₇₃₀; (c) Relative chlorophyll content of wild type and mutant; (d) The 77 K fluorescence emission spectra of wild type and mutant with excitation at 435 nm. Spectra were normalized to emission at 725 nm.

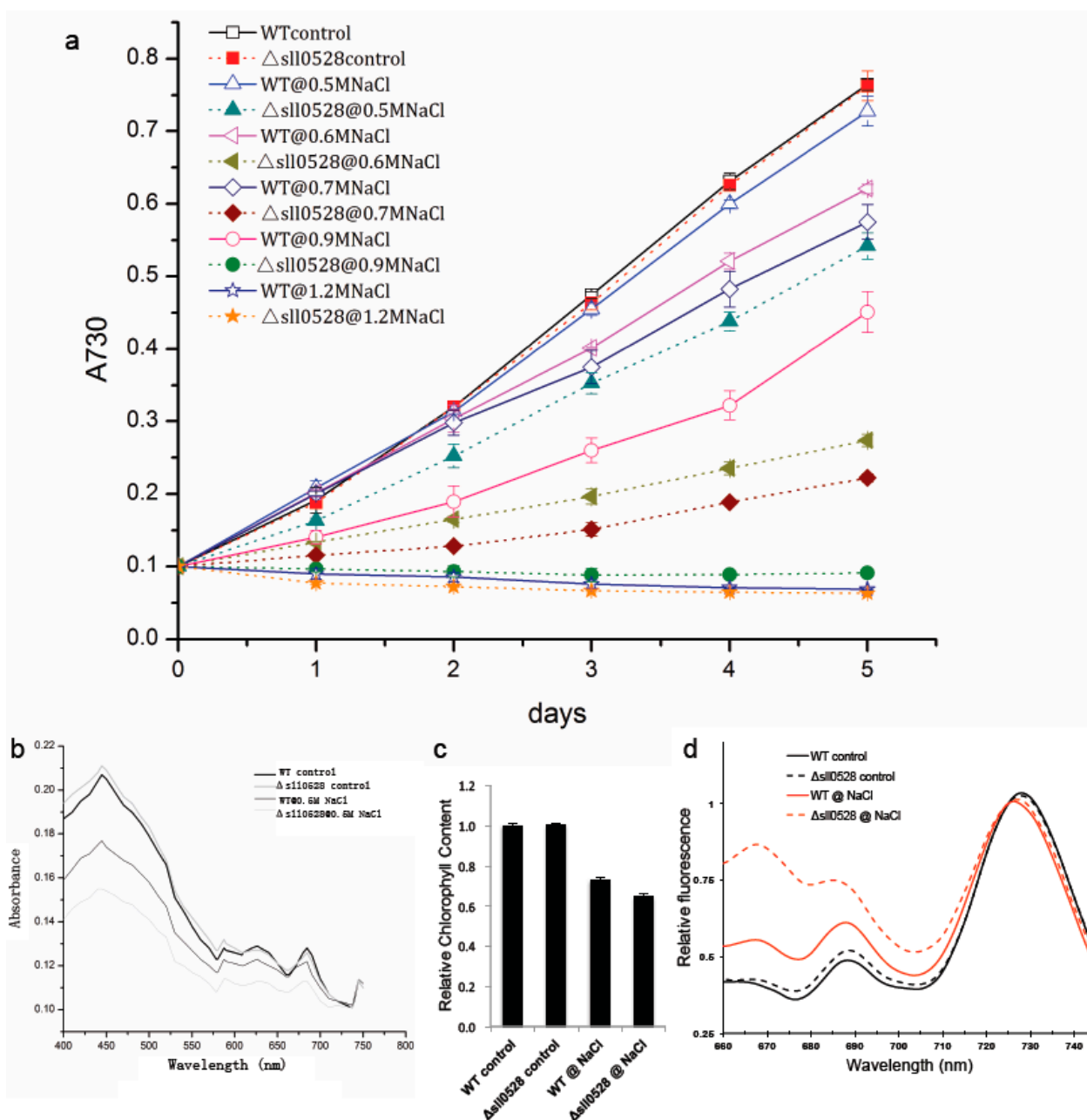
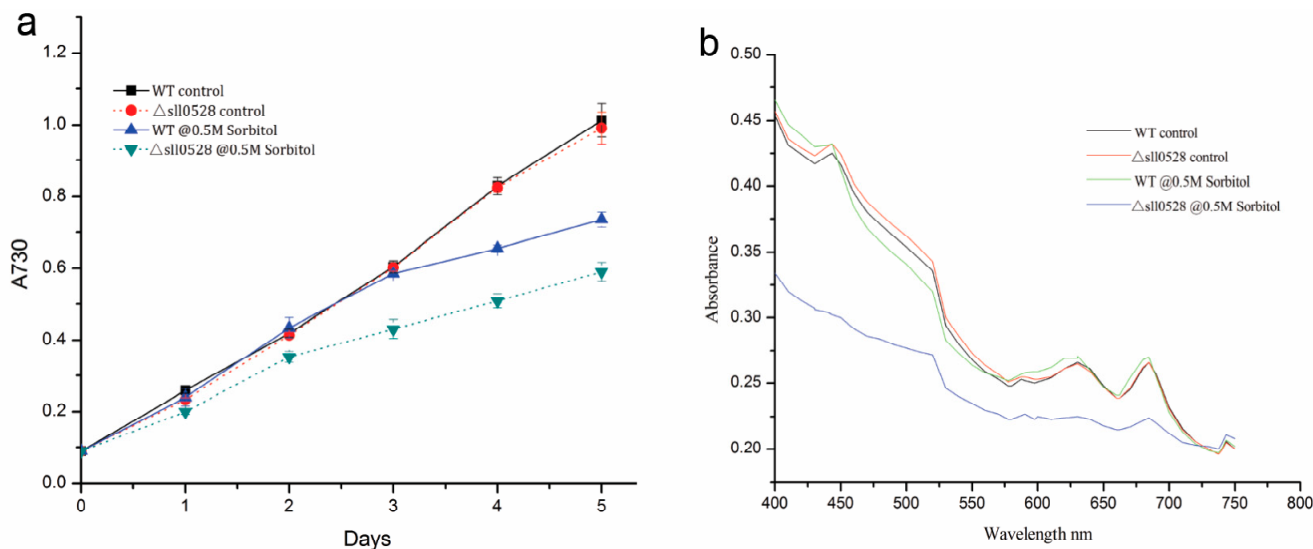


Figure 4. Increased sensitivity of *sll0528* mutant to hyperosmotic stress generated by sorbitol. **(a)** Growth curve of wild type (WT) and *sll0528* mutant ($\Delta sll0528$) under 0.5 M sorbitol. Initial OD₇₃₀ was 0.1. Each data point represents the mean of at least three independent biological replicates, and the error bars denote SD; **(b)** Absorption spectra of wild type and *sll0528* mutant 24 h after transferred to 0.5 M sorbitol, normalized to OD₇₃₀.



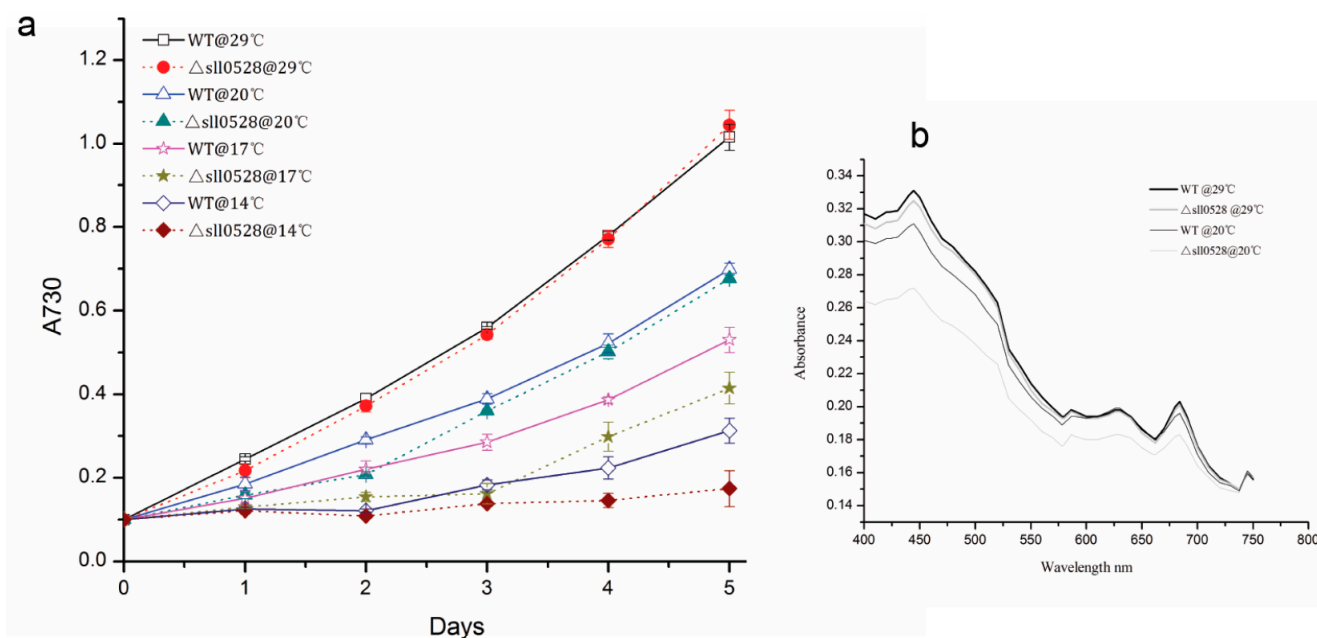
2.3.3. Sll0528 Is Crucial for Cold Acclimation

The growth rate of wild type decreased gradually when the temperature decreased from 29 to 14 °C. As compared to wild type, the *sll0528* mutant had a delayed or disrupted cold acclimation (Figure 5a). Under 20 °C, the *sll0528* mutant grew more slowly than wild type during the first two days, but it caught up with wild type from the third day and had a similar growth rate with wild type on the fourth and fifth days. The whole-cell absorption spectra of wild type and mutant 24 h after being transferred to 20 °C indicates the distinct variation in the mutant (Figure 5b). Compared to the slight reduction of chlorophyll and carotenoids in wild type upon cold stress, a remarkable decrease of chlorophyll, carotenoids and phycocyanin in mutant upon cold stress suggested severely impaired photosystems. These defects were correlated with its retarded cell growth. Under lower temperature such as 17 °C, no significant growth was observed in the mutant during the first three days, but it resumed growth from the third day and had similar growth rate as wild type on the fourth and fifth days, though the cell density was still lower than wild type. At 14 °C, no propagation of wild type or mutant was detected in the first two days. Wild type resumed growth slightly on the third day, and significant growth was detected on the fourth and fifth days. However, the mutant could hardly recover during the five days of our observation. Thus, such postponed or disrupted cold acclimation in the *sll0528* mutant implied its reduction in cold resistance, and suggested the functional Sll0528 protein was essential for efficient cold acclimation.

At lower temperature, *Synechocystis* activated the expression of the fatty acid desaturases gene and enhanced membrane lipid unsaturation to ensure membrane fluidity [27–29]. Further, histidine kinase Hik33 was an important sensor of cold stress, which might sense the membrane fluidity [30,31]. RNA-binding protein 1 (Rbp1) and RNA helicase (CrhR) were recently reported to play indispensable roles in cold acclimation [32–36]. Whether the membrane fluidity and the extent of membrane lipid

unsaturation of *sll0528* mutant were different from wild type upon cold stress needs to be further investigated. Also, exploration of the relationships between Sll0528 and Hik33, as well as Rbp1 and CrhR might help to sketch the picture of cold acclimation in *Synechocystis*.

Figure 5. Increased sensitivity of *sll0528* mutant to cold stress. **(a)** Growth curve of wild type (WT) and *sll0528* mutant ($\Delta sll0528$) at different temperatures. Significant differences were observed between the mutant and wild type at the 2nd day upon 20 °C, from the 2nd to 5th day upon 17 °C and at the 4th and 5th day upon 14 °C respectively ($p < 0.05$). Initial OD₇₃₀ was 0.1 when the temperature was changed. Each data point represents the mean of at least three independent biological replicates, and the error bars denote SD; **(b)** Absorption spectra of wild type and *sll0528* mutant 24 h after transferred to 20 °C, normalized to OD₇₃₀.



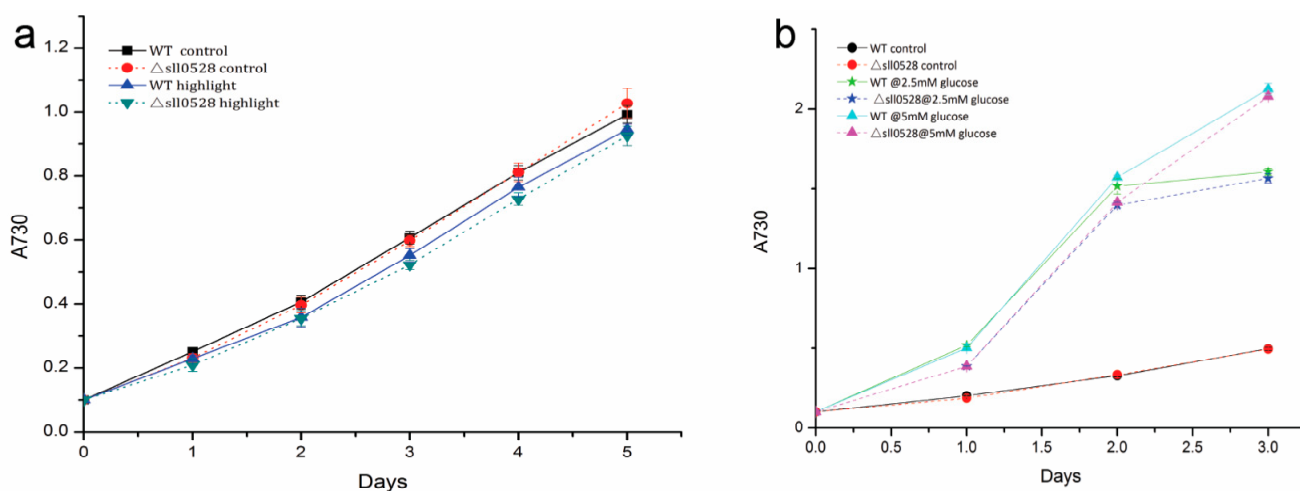
2.3.4. Sll0528 Is Dispensable for Acclimation to High Light and Mixotrophic Growth

The *sll0528* mutant had a growth rate similar with wild type under continuous illumination of $30 \mu\text{mol}\cdot\text{m}^{-2}\cdot\text{s}^{-1}$. The growth rate of both wild type and *sll0528* mutant was slightly decreased under higher light illumination of $150 \mu\text{mol}\cdot\text{m}^{-2}\cdot\text{s}^{-1}$. But the decrease was not significant and there is no notable difference between wild type and the *sll0528* mutant (Figure 6a).

Under mixotrophic growth condition, glucose was found to accelerate growth of wild type and the *sll0528* mutant remarkably (Figure 6b). As to wild type, glucose of 2.5 or 5 mM doubled the OD₇₃₀ at 24 h, and tripled its OD₇₃₀ at 48 h. After 48 h, the growth rate under 2.5 mM glucose slowed down and was similar with control under autotrophic growth, while the growth rate under 5 mM glucose still surpassed autotrophic control. This might be due to the exhaustion of glucose under 2.5 mM, but not 5 mM glucose. As for the *sll0528* mutant, it had a similar accelerated growth pattern as wild type under mixotrophic growth condition. Though its growth rate was slightly lower than wild type under 2.5 and 5 mM glucose, the difference was not significant (Figure 6b).

The similarity of response to high light and mixotrophic growth condition in the *sll0528* mutant and wild type suggested that although the *sll0528* gene was induced (Figure 1d,e), the Sll0528 protein was dispensable for these conditions.

Figure 6. (a) Growth curve of wild type (WT) and *sll0528* mutant ($\Delta sll0528$) in continuous light of control ($30 \mu\text{mol}\cdot\text{m}^{-2}\cdot\text{s}^{-1}$) and high light ($150 \mu\text{mol}\cdot\text{m}^{-2}\cdot\text{s}^{-1}$); (b) Growth curves of wild type and *sll0528* mutant under mixotrophic growth condition with different concentration of glucose. Initial OD₇₃₀ was 0.1 when the condition was changed. Each data point represents the mean of at least three independent biological replicates, and the error bars denote SD.



2.4. Recombinant Sll0528 Has Proteolytic Activity

To further investigate the proteolytic activity of Sll0528, a GST-Sll0528 construct was generated and expressed in *E. coli*. The recombinant GST-Sll0528 protein was purified and tested against beta-casein. Beta-casein was cleaved into smaller fragments time-dependently when incubated with GST-Sll0528 (Figure 7). Beta-casein could not be digested by another GST recombinant protein P. It indicated that the protease activity was from GST-Sll0528, but not a contaminant from the expression system. This proteolytic activity was not inhibited by Complete EDTA-free (a cocktail of serine and cysteine protease inhibitors), but was inhibited by *o*-phenanthroline (a metal chelator), suggesting that Sll0528 might function as a metalloprotease in *Synechocystis*.

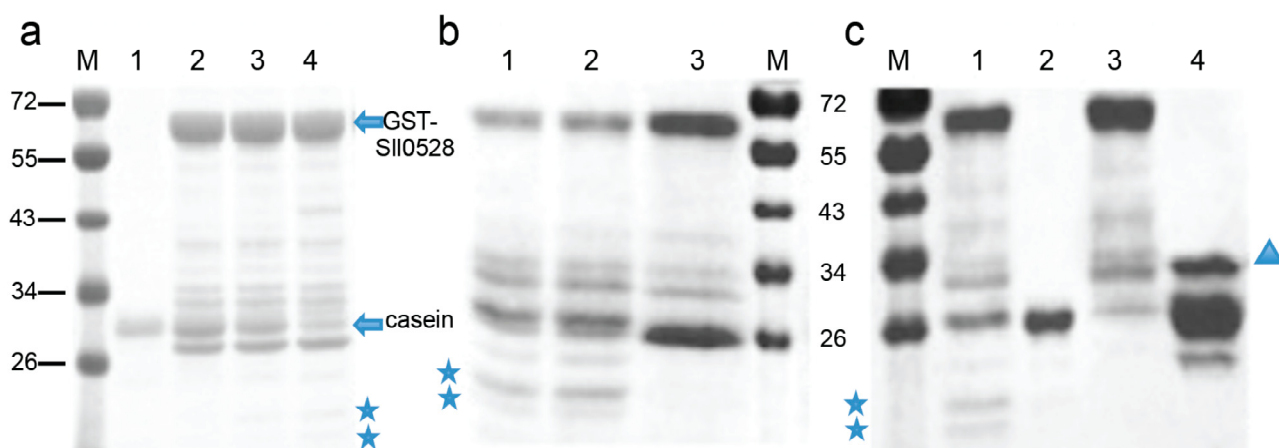
3. Experimental Section

3.1. Strains, Culture and Stress Conditions

Derived from ATCC27184, *Synechocystis* sp. PCC 6803 was cultivated in BG11 medium and illuminated with $30 \mu\text{mol}\cdot\text{photons}\cdot\text{m}^{-2}\cdot\text{s}^{-1}$ at 30°C as optimum condition. Cultures were buffered with 20 mM HEPES-NaOH (pH 7.5), with oscillation at 130 rpm. The stress conditions used in RT-qPCR were as follows: salt stress (5% NaCl, 854 mM); cold stress (4°C with light illumination); hyperosmotic stress (0.5 M sorbitol); high light ($200 \mu\text{mol}\cdot\text{photons}\cdot\text{m}^{-2}\cdot\text{s}^{-1}$); mixotrophic growth condition (2.5 mM glucose). Samples of 30 mL before the stress (0 h) and after timely intervals of

0.25, 0.5, 1, 2, 4 and 6 h were collected. Harvested cells were washed once in 1.6 mL of TE (pH 8.0) and centrifuged at 12,000 rpm at 4 °C for 5 min. The cell pellets were immediately frozen in liquid nitrogen and stored at –80 °C until they were used for RNA isolation.

Figure 7. *In vitro* protease activity of recombinant SII0528. **(a)** The time-dependent proteolytic activity of recombinant SII0528. Lane 1, the substrate beta-casein remained intact in the reaction buffer after 15 h of incubation. Lane 2, reaction mixture of GST-SII0528 and beta-casein prior to incubation. Lanes 3 and 4, incubated with GST-SII0528 for 5 and 15 h, the substrate beta-casein was cleaved significantly. Stars indicated the cleaved fragments of beta-casein; **(b)** The inhibitor study. Lane 1, GST-SII0528 cleaved beta-casein significantly after 15 h incubation. Lane 2, the proteolytic activity of SII0528 was not inhibited by Complete EDTA-free (a cocktail of serine and cysteine protease inhibitors). Lane 3, the proteolytic activity of SII0528 was inhibited by 10 mM *o*-phenanthroline; **(c)** The comparison of proteolytic activity to the recombinant protein P. Lane 1, GST-SII0528 cleaved beta-casein significantly after 15 h incubation. Lane 2, the substrate beta-casein remained intact in the reaction buffer after 15 h of incubation. Lane 3, purified GST-SII0528 in the reaction buffer after 15 h incubation. Lane 4, reaction mixture of beta-casein and GST-recombinant protein P (indicated by triangle).



3.2. RNA Isolation and Quantitative RT-PCR

Total RNA was extracted according to the instructions of the RNA extraction kit (DongSheng Biotech, Guangzhou, China) with modification, as previously described [12]. The DNA residue was removed by DNase and DNA contamination was tested by PCR reaction without reverse transcription. Quantitative RT-PCR was performed using one-step SYBR Green I kit (TAKARA Biotech, Dalian, China) on ABI7500 (Life Technologies, Grand Island, NY, USA) using the following conditions: reverse transcription program as 42 °C for 5 min, 95 °C for 10 s; amplification and quantification program repeated for 40 cycles of 95 °C for 5 s, 60 °C for 34 s; melting curve program as 95 °C for 15 s, 60 °C for 1 min and 95 °C for 15 s. The *rnpB* gene that encodes subunit B of ribonuclease P was used as an internal control. The primers sets of S2Ps were listed in Table 1. Melting curve analysis was performed after each run to confirm the homogeneity in the amplification. Three independent biological replicates for each sample and three technical replicates of each biological replicate were

analyzed. For the reactions, a master mix of the following components was prepared: 10 μL 2 \times One step SYBR RT-PCR Buffer, 3.2 μL RNase-Free H_2O , 0.8 μL (0.4 μM) forward primer, 0.8 μL (0.4 μM) reverse primer, 0.8 μL PrimeScript one-step enzyme mix, 0.4 μL ROX, 4 μL total RNA. The relative expression of genes was calculated using $2^{-\Delta\Delta\text{Ct}}$ method [37].

3.3. Construction of *sll0528* Mutant

The downstream and upstream fragments of *sll0528* gene were amplified from wild-type *Synechocystis* genomic DNA with primer pairs as indicated in Figure 2 and Table 1, P1 and P2, P3 and P4 respectively. The PCR fragments digested with XhoI and SacI or BamHI and NdeI (sites underlined in primer sequences) were inserted into the XhoI-SacI or BamHI-NdeI site of pET-30b (+) to generate p0528. The chloramphenicol resistance cassette was amplified from pACYC184 with primer P5 and P6. It was digested with SacI and BamHI, and inserted into the SacI-BamHI site of p0528 to yield pC0528, which was used to transform *Synechocystis*. Chloramphenicol of 40 $\mu\text{g}\cdot\text{mL}^{-1}$ was added for the selection of *sll0528* mutant. The complete replacement of *sll0528* coding region was verified with primers P7 and P8.

3.4. Measurement of Physiological Parameters

The growth curve of wild type and mutant was prepared by measuring OD₇₃₀ every 24 h during the first three or five days. Whole cell absorbance was measured 24 h after stress condition (unless otherwise specified) by using a UV2300 spectrophotometer (Techcomp, Beijing, China) scanning from 400 to 750 nm. Extraction and measurement of chlorophyll were performed as described previously [38]. Chlorophyll fluorescence at 77 K was measured as described previously [39] with an LS-55 fluorescence spectrometer (PerkinElmer, Waltham, MA, USA).

3.5. Expression of Recombinant Sll0528 and in Vitro Proteolytic Activity Assay

The coding sequence of Sll0528 was amplified using primers P9 and P10. The fragment was cloned into pGEX-2T to generate a GST-Sll0528 fusion protein. This construct was expressed in *E. coli* strain BL21(DE3)pLysS and recombinant GST-Sll0528 was purified through GST affinity column (Sigma-Aldrich, St. Louis, MO, USA). The proteolytic activity assay was conducted against 1 or 2 μg beta-casein in a reaction buffer containing 50 mM Tris-acetate (pH 8.0), 80 mM NaCl, 5 mM Mg-acetate and 12.5 μM Zn-acetate. Quantification of casein was performed by ImageJ on the Coomassie brilliant blue R250 stained gel.

3.6. Data Analysis

Relative expression levels were determined after normalization with the *rnpB* transcript level using ABI7500 SDS software version 4.0 (Life Technologies, Grand Island, NY, USA). The average relative expression levels and standard deviations were determined from the data generated in independent experiments. One way ANOVA was performed by SPSS software to determine the significance of the relative expression ratios, $p < 0.05$ was considered significant.

Table 1. Primers used in this research. The restriction enzyme cleavage sites were underlined.

Primer Name	Sequence of Primer (5'-3')
sll0528-L	GGAAGCCTTTACTGCTGAAGAT
sll0528-R	TGTCGGCACCAATAACCAAG
sll0862-L	GGCAAATGCGGGAAGAAG
sll0862-R	TGTCACCGAGCACAGTGGT
slr0643-L	GGTTTGTCCACTGCTCTACT
slr0643-R	GGCTGTGATGATTTCTGC
slr1821-L	TTGGATGGTGGGCAATTG
slr1821-R	ATACCCCTAAGCTCAGCAGAAG
rnpB-L	CCACTGAAAAGGGTAAGGG
rnpB-R	CTCCGACCTTGCTTCCA
P1	<u>CGAGCTCCTAC</u> GGAAGACATCAAACACG
P2	CCGCTCGAGGGCGAAATGTTGACCTTGAC
P3	GGAATTC <u>CATATG</u> CTGGTTATGGTGGTTTACTGA
P4	CGCGGATCCATGTTAAGAATTGCCTGAGTG
P5	CGCGGATCCTCATCAGTGCCAACATAG
P6	<u>CGAGCTCGG</u> TAAACCAGCAATAGACAT
P7	CAAGTACAC CTAACAGTTGA
P8	ATGTAAAGCCTCAGTTTAG
P9	CGCGGATCCATGTTAAGCCTCAGTTTAGGGG
P10	CCGGAATTCCTAGGCGGCGGAGGTTTGCAG

4. Conclusions

In conclusion, the *sll0528* gene was highly induced by salt, cold and hyperosmotic stress and its knockout mutant displayed increased sensitivity to salt, cold and hyperosmotic stress. The recombinant Sll0528 protein was a metalloprotease as its homologs in other organisms. Results here provided the first evidence that Sll0528, a Site-2-protease in *Synechocystis* sp. PCC 6803 is crucial for salt, cold and hyperosmotic stress acclimation. Further investigation of its mechanism will hopefully shed light on the mechanisms of stress acclimation in cyanobacteria.

Acknowledgments

This work was supported by grants 30800609, 31270085 awarded to Gu Chen from National Natural Science Foundation of China. It was also partly supported by grants 31370383 awarded to Dong Wei from National Natural Science Foundation of China.

Author Contributions

Haijin Lei, Yuling Wang and Gu Chen conceived and designed the experiments; Haijin Lei, Yuling Wang, Qinglong Ding performed the experiments; Haijin Lei, Yuling Wang and Gu Chen analyzed the data; Dong Wei contributed reagents, materials and analysis tools; Haijin Lei, Yuling Wang and Gu Chen wrote the manuscript.

Conflicts of Interest

The authors declare no conflict of interest.

References

1. Guerrero, F.; Carbonell, V.; Cossu, M.; Correddu, D.; Jones, P.R. Ethylene synthesis and regulated expression of recombinant protein in *Synechocystis* sp. PCC 6803. *PLoS One* **2012**, *7*, e50470.
2. Liu, X.; Sheng, J.; Curtiss, R., III. Fatty acid production in genetically modified cyanobacteria. *Proc. Natl. Acad. Sci. USA* **2011**, *108*, 6899–6904.
3. Oliver, J.W.; Machado, I.M.; Yoneda, H.; Atsumi, S. Cyanobacterial conversion of carbon dioxide to 2,3-butanediol. *Proc. Natl. Acad. Sci. USA* **2013**, *110*, 1249–1254.
4. Los, D.A.; Zorina, A.; Sinetova, M.; Kryazhov, S.; Mironov, K.; Zinchenko, V.V. Stress sensors and signal transducers in cyanobacteria. *Sensors* **2010**, *10*, 2386–2415.
5. Chen, G.; Zhang, X. New insights into S2P signaling cascades: Regulation, variation, and conservation. *Pro. Sci.* **2010**, *19*, 2015–2030.
6. Brown, M.S.; Goldstein, J.L. The SREBP pathway: Regulation of cholesterol metabolism by proteolysis of a membrane-bound transcription factor. *Cell* **1997**, *89*, 331–340.
7. Brown, M.S.; Goldstein, J.L. A proteolytic pathway that controls the cholesterol content of membranes, cells, and blood. *Proc. Natl. Acad. Sci. USA* **1999**, *96*, 11041–11048.
8. Brown, M.S.; Ye, J.; Rawson, R.B.; Goldstein, J.L. Regulated intramembrane proteolysis: Review a control mechanism conserved from bacteria to humans. *Cell* **2000**, *100*, 391–398.
9. Chen, G.; Bi, Y.R.; Li, N. EGY1 encodes a membrane-associated and ATP-independent metalloprotease that is required for chloroplast development. *Plant J. Cell Mol. Biol.* **2005**, *41*, 364–375.
10. Chen, G.; Law, K.; Ho, P.; Zhang, X.; Li, N. EGY2, a chloroplast membrane metalloprotease, plays a role in hypocotyl elongation in Arabidopsis. *Mol. Biol. Rep.* **2012**, *39*, 2147–2155.
11. Chen, G.; Wen, P.P.; Qin, C.; Wang, Y. Expression of green fluorescent protein-tagged S2P homologs in *Synechocystis* sp. PCC 6803. *J. South China Uni. Technol.* **2012**, *40*, 122–127.
12. Zhang, X.; Chen, G.; Qin, C.; Wang, Y.; Wei, D. Slr0643, an S2P homologue, is essential for acid acclimation in the cyanobacterium *Synechocystis* sp. PCC 6803. *Microbiology* **2012**, *158*, 2765–2780.
13. Guo, D.; Gao, X.R.; Li, H.; Zhang, T.; Chen, G.; Huang, P.B. EGY1 plays a role in regulation of endodermal plastid size and number that are involved in ethylene-dependent gravitropism of light-grown Arabidopsis hypocotyls. *Plant Mol. Biol.* **2008**, *66*, 345–360.
14. Chen, K.; Gu, L.; Xiang, X.; Lynch, M.; Zhou, R. Identification and characterization of five intramembrane metalloproteases in *Anabaena variabilis*. *J. Bacteriol.* **2012**, *194*, 6105–6115.
15. Kanasaki, Y.; Suzuki, I.; Allakhverdiev, S.I.; Mikami, K.; Murata, N. Salt stress and hyperosmotic stress regulate the expression of different sets of genes in *Synechocystis* sp. PCC 6803. *Biochem. Biophys. Res. Commun.* **2002**, *290*, 339–348.

16. Marin, K.; Kanesaki, Y.; Los, D.A.; Murata, N.; Suzuki, I.; Hagemann, M. Gene expression profiling reflects physiological processes in salt acclimation of *Synechocystis* sp. strain PCC 6803. *Plant Physiol.* **2004**, *136*, 3290–3300.
17. Shoumskaya, M.A.; Paithoonrangsarid, K.; Kanesaki, Y.; Los, D.A.; Zinchenko, V.V.; Tanticcharoen, M. Identical Hik-Rre systems are involved in perception and transduction of salt signals and hyperosmotic signals but regulate the expression of individual genes to different extents in *synechocystis*. *J. Biol. Chem.* **2005**, *280*, 21531–21538.
18. Shapiguzov, A.; Lyukevich, A.A.; Allakhverdiev, S.I.; Sergeyenko, T.V.; Suzuki, I.; Murata, N. Osmotic shrinkage of cells of *Synechocystis* sp. PCC 6803 by water efflux via aquaporins regulates osmostress-inducible gene expression. *Microbiology* **2005**, *151*, 447–455.
19. Paithoonrangsarid, K.; Shoumskaya, M.A.; Kanesaki, Y.; Satoh, S.; Tabata, S.; Los, D.A. Five histidine kinases perceive osmotic stress and regulate distinct sets of genes in *Synechocystis*. *J. Biol. Chem.* **2004**, *279*, 53078–53086.
20. Inaba, M.; Suzuki, I.; Szalontai, B.; Kanesaki, Y.; Los, D.A.; Hayashi, H. Gene-engineered rigidification of membrane lipids enhances the cold inducibility of gene expression in *Synechocystis*. *J. Biol. Chem.* **2003**, *278*, 12191–12198.
21. Kanesaki, Y.; Shiwa, Y.; Tajima, N.; Suzuki, M.; Watanabe, S.; Sato, N. Identification of substrain-specific mutations by massively parallel whole-genome resequencing of *Synechocystis* sp. PCC 6803. *DNA Res.* **2012**, *19*, 67–79.
22. Danika, T.; Bjorn, V.; Annegret, W.; Salim, A.; Wolfgang, R.H. Microevolution in cyanobacteria: Re-sequencing a motile substrain of *Synechocystis* sp PCC 6803. *DNA Res.* **2012**, *19*, 435–448.
23. Tajima, N.; Sato, S.; Maruyama, F.; Kaneko, T.; Sasaki, N.V.; Kurokawa, K. Genomic structure of the cyanobacterium *Synechocystis* sp PCC 6803 strain GT-S. *DNA Res.* **2011**, *18*, 393–399.
24. Hagemann, M. Molecular biology of cyanobacterial salt acclimation. *FEMS Microbiol. Rev.* **2011**, *35*, 87–123.
25. Jittawuttipoka, T.; Planchon, M.; Spalla, O.; Benzerara, K.; Guyot, F.; Cassier-Chauvat, C. Multidisciplinary evidences that *Synechocystis* PCC6803 exopolysaccharides operate in cell sedimentation and protection against salt and metal stresses. *PLoS One* **2013**, *8*, e55564.
26. Nikkinen, H.L.; Hakkila, K.; Gunnelius, L.; Huokko, T.; Pollari, M.; Tyystjarvi, T. The SigB σ factor regulates multiple salt acclimation responses of the cyanobacterium *Synechocystis* sp. PCC 6803. *Plant Physiol.* **2012**, *158*, 514–523.
27. Los, D.A.; Ray, M.K.; Murata, N. Differences in the control of the temperature-dependent expression of four genes for desaturases in *Synechocystis* sp. PCC 6803. *Mol. Microbiol.* **1997**, *25*, 1167–1175.
28. Mironov, K.S.; Sidorov, R.A.; Trofimova, M.S.; Bedbenov, V.S.; Tsydendambaev, V.D.; Allakhverdiev, S.I. Light-dependent cold-induced fatty acid unsaturation, changes in membrane fluidity, and alterations in gene expression in *Synechocystis*. *Biochim. Biophys. Acta* **2012**, *1817*, 1352–1359.
29. Wada, H.; Murata, N. Temperature-induced changes in the fatty acid composition of the cyanobacterium, *Synechocystis* PCC6803. *Plant Physiol.* **1990**, *92*, 1062–1069.
30. Suzuki, I.; Kanesaki, Y.; Mikami, K.; Kanehisa, M.; Murata, N. Cold-regulated genes under control of the cold sensor Hik33 in *Synechocystis*. *Mol. Microbiol.* **2001**, *40*, 235–244.

31. Suzuki, I.; Los, D.A.; Kanesaki, Y.; Mikami, K.; Murata, N. The pathway for perception and transduction of low-temperature signals in *Synechocystis*. *EMBO J.* **2000**, *19*, 1327–1334.
32. Prakash, J.S.; Krishna, P.S.; Sirisha, K.; Kanesaki, Y.; Suzuki, I.; Shivaji, S. An RNA helicase, CrhR, regulates the low-temperature-inducible expression of heat-shock genes groES, groEL1 and groEL2 in *Synechocystis* sp. PCC 6803. *Microbiology* **2010**, *156*, 442–451.
33. Rosana, A.R.; Ventakesh, M.; Chamot, D.; Patterson-Fortin, L.M.; Tarassova, O.; Espie, G.S. Inactivation of a low temperature-induced RNA helicase in *Synechocystis* sp. PCC 6803: Physiological and morphological consequences. *Plant Cell Physiol.* **2012**, *53*, 646–658.
34. Rowland, J.G.; Simon, W.J.; Prakash, J.S.; Slabas, A.R. Proteomics reveals a role for the RNA helicase crhR in the modulation of multiple metabolic pathways during cold acclimation of *Synechocystis* sp. PCC6803. *J. Proteome. Res.* **2011**, *10*, 3674–3689.
35. Sireesha, K.; Radharani, B.; Krishna, P.S.; Sreedhar, N.; Subramanyam, R.; Mohanty, P. RNA helicase, CrhR is indispensable for the energy redistribution and the regulation of photosystem stoichiometry at low temperature in *Synechocystis* sp PCC6803. *Biochim. Biophys. Acta Bioenerg.* **2012**, *1817*, 1525–1536.
36. Tan, X.; Zhu, T.; Shen, S.; Yin, C.; Gao, H.; Xu, X. Role of Rbp1 in the acquired chill-light tolerance of cyanobacteria. *J. Bacteriol.* **2011**, *193*, 2675–2683.
37. Livak, K.J.; Schmittgen, T.D. Analysis of relative gene expression data using real-time quantitative PCR and the $2^{-\Delta\Delta C_t}$ method. *Methods* **2001**, *25*, 402–408.
38. Hartmut, K.L. Chlorophylls and carotenoids: Pigments of photosynthetic biomembranes. In *Methods in Enzymology*; Academic Press: Waltham, MA, USA, 1987; pp. 350–382.
39. Kondo, K.; Ochiai, Y.; Katayama, M.; Ikeuchi, M. The membrane-associated CpcG2-phycoobilisome in *Synechocystis*: A new photosystem I antenna. *Plant Physiol.* **2007**, *144*, 1200–1210.

© 2014 by the authors; licensee MDPI, Basel, Switzerland. This article is an open access article distributed under the terms and conditions of the Creative Commons Attribution license (<http://creativecommons.org/licenses/by/4.0/>).